Published online 15 December 2007

Nucleic Acids Research, 2008, Vol. 36, No. 2 ***697–704***
doi:10.1093/nar/gkm1088

Studies on the mechanism of inhibition of bacterial ribonuclease P by aminoglycoside derivatives

Steven A. Kawamoto, Christopher G. Sudhahar, Cynthia L. Hatfield, Jing Sun, Edward J. Behrman and Venkat Gopalan*

Department of Biochemistry, The Ohio State University, Columbus, OH 43210, USA

Received October 10, 2007; Revised November 19, 2007; Accepted November 20, 2007

ABSTRACT

Ribonuclease P (RNase P) is a Mg^{2+}-dependent endoribonuclease responsible for the 5′-maturation of transfer RNAs. It is a ribonucleoprotein complex containing an essential RNA and a varying number of protein subunits depending on the source: at least one, four and nine in Bacteria, Archaea and Eukarya, respectively. Since bacterial RNase P is required for viability and differs in structure/subunit composition from its eukaryal counterpart, it is a potential antibacterial target. To elucidate the basis for our previous finding that the hexa-arginine derivative of neomycin B is 500-fold more potent than neomycin B in inhibiting bacterial RNase P, we synthesized hexa-guanidinium and -lysyl conjugates of neomycin B and compared their inhibitory potential. Our studies indicate that side-chain length, flexibility and composition cumulatively account for the inhibitory potency of the aminoglycoside-arginine conjugates (AACs). We also demonstrate that AACs interfere with RNase P function by displacing Mg^{2+} ions. Moreover, our finding that an AAC can discriminate between a bacterial and archaeal (an experimental surrogate for eukaryal) RNase P holoenzyme lends promise to the design of aminoglycoside conjugates as selective inhibitors of bacterial RNase P, especially once the structural differences in RNase P from the three domains of life have been established.

INTRODUCTION

In the search for new therapeutic strategies to help reduce or eliminate viral and bacterial infections, RNAs and RNA-protein (RNP) complexes have come to the fore as promising targets by virtue of their central roles in key cellular processes (1–4). Ribonuclease P (RNase P), a catalytic RNP complex (5–8), is one such example that has attracted consideration as an antibacterial target (9,10). RNase P is a Mg^{2+}-dependent endoribonuclease primarily involved in 5′-maturation of tRNAs in all three domains of life (Figure 1). However, there are notable differences in its structure and subunit composition depending on the source (5–8). All RNase P holoenzymes are RNPs made up of an essential RNase P RNA (RPR) and a variable number of RNase P Protein (RPP) subunits: at least one, four and nine in Bacteria, Archaea and Eukarya, respectively. The observations that bacterial RNase P (i) is essential for viability, (ii) is present in low copy number and (iii) differs in structure/subunit composition from its eukaryal counterpart, have justified studies to identify inhibitors of its activity (9,10).

Aminoglycosides (AGs) are naturally occurring, cationic pseudo-oligo-saccharides that impair translational fidelity by binding the A-site in the bacterial 16S rRNA (11–13). This finding provided the impetus to examine the ability of AGs, with an established history as antibacterial agents, to interfere with the function of other RNAs (13,14). Indeed, various catalytic RNAs, including the RNA moiety of bacterial RNase P, are inhibited by AGs like neomycin and kanamycin (15–17). Various experimental and computational studies on the mode of action of AGs have revealed that the ability of AGs to interact with several unrelated RNAs is due to their (i) multiple positive charges that allow them to engage in electrostatic interactions with RNAs, (ii) potential for hydrogen bonding and (iii) conformational flexibility that permits induced fit, which is often observed during RNA-ligand interactions (13,18–20). Moreover, the striking coincidence between the NH_3^+–NH_3^+ distances in the AGs and the Mg^{2+}–Mg^{2+} distances in the hammerhead ribozyme (as revealed by molecular dynamics calculations) furnished a structural basis for understanding how AGs can readily displace metal ions and interfere with the function of a target RNA (18).

Despite the ability of AGs to alter the function of different RNAs, their promiscuity as ligands stimulated

*To whom correspondence should be addressed. Tel: +1 614 292 1332; Fax: +1 614 292 6773; Email: gopalan.5@osu.edu

The authors wish it to be known that, in their opinion, the first three authors should be regarded as joint First Authors.

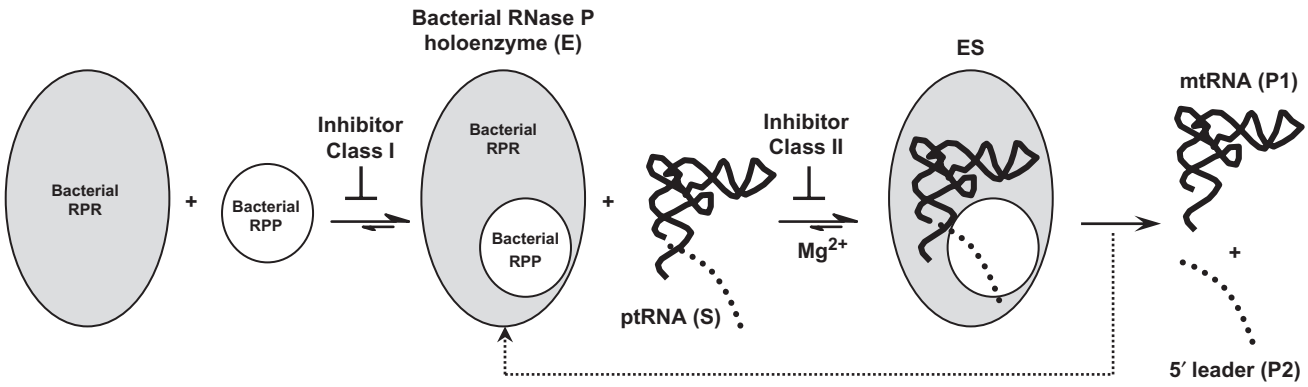

Figure 1. A depiction of the assembly of the bacterial RNase P holoenzyme and its subsequent catalysis of ptRNA processing. The two broad classes of potential inhibitors of bacterial RNase P and their sites of interference are indicated. This figure is adapted from an illustration in Christian *et al.* (49).

studies to modify the AGs and thereby impart greater selectivity while maintaining the affinity for a desired target RNA (13). An elegant illustration in this regard was the guanidinylation of AGs that resulted in enhanced discrimination among RNAs (21). Since RNA-binding proteins utilize Arg-rich sequences for RNA recognition (22,23), Lapidot and coworkers conjugated Arg residues to neomycin B (NeoB), gentamycin or kanamycin backbones to construct aminoglycoside-arginine conjugates (AACs) with the expectation that these compounds will act as potent and selective peptidomimetics that would prevent RNP assembly (24,25). Indeed, AACs were proven to be effective antagonists of the HIV Tat-TAR RNA interaction. Our earlier investigation of AACs also revealed that the hexa-arginine derivative of neomycin B (NeoR6) was nearly 500-fold more potent than NeoB in inhibiting bacterial RNase P and that NeoR6 was not as effective against human RNase P (26). In this report, we describe our efforts to examine structure-activity relationships in AG-based inhibitors and to determine their mechanism of inhibition of RNase P.

MATERIALS AND METHODS

Synthesis of AG derivatives

Reagent-grade solvents and distilled H_2O were used without further purification unless otherwise stated. The progress of reactions was monitored by thin layer chromatography (using either UV or ninhydrin-based detection) or electrospray ionization mass spectrometry (ESI MS). Compounds were purified by either flash column (silica gel, 200–400 mesh) or ion-exchange chromatography and were subsequently desalted by size-exclusion chromatography. Purified compounds were characterized by ^{1}H and ^{13}C NMR spectroscopy, FT-IR spectroscopy, ESI-Q-TOF MS, LCT-TOF MS (Campus Chemical Instrument Center, The Ohio State University), C, H, N elemental analysis (QTI, Inc., Whitehouse, NJ, USA) and Karl Fisher coulombic titration (QTI, Inc., Whitehouse, NJ, USA). A complete description of the methods used for synthesis is provided elsewhere (27, 'Supplementary Data').

RNase P activity assays in the absence and presence of inhibitors

Archaeal/bacterial RPRs and precursor $tRNA^{Tyr}$ ($ptRNA^{Tyr}$) were prepared by run-off *in vitro* transcription using T7 RNA polymerase (28–31). RPRs, in water, were folded according to the protocol outlined by Zahler *et al.* (32). Bacterial and archaeal RNase P holoenyzmes were reconstituted *in vitro* using their respective RPR and RPP recombinant subunits. While *Escherichia coli* RNase P served as the bacterial prototype, *Methanothermobacter thermautotrophicus* (*Mth*) and *Methanocaldococcus jannaschii* (*Mja*) RNase P were used as the archaeal representatives.

Bacterial and archaeal RNase P activities were measured in the absence and presence of various concentrations of inhibitors. Time-course assays were performed to determine the initial velocities. All assays were performed under multiple-turnover conditions using $ptRNA^{Tyr}$ as the substrate. In general, the order of additions was as follows. The corresponding RPR and RPP(s) were pre-incubated (~10 min) at the respective assay temperature to allow holoenzyme assembly prior to a 5-min incubation with the appropriate inhibitor. In rescue experiments, either Mg^{2+} or RPP (in excess of that used for holoenzyme generation) was added after addition of the inhibitor. Reactions (10 μL) were initiated by addition of radiolabeled $ptRNA^{Tyr}$ and terminated after a defined time period using 9 μL of quench dye [0.05% (w/v) bromophenol blue, 0.05% (w/v) xylene cyanol, 10 mM EDTA, 7 M urea] and 1 μL phenol. Bacterial RNase P reactions were performed at 37°C either in a 'high-salt' buffer [10 mM HEPES, 10 mM $Mg(CH_3CO_2)_2$, 400 mM $NH_4CH_3CO_2$, 5% (v/v) glycerol, and 0.01% (v/v) IGEPAL, pH 7.2] or a 'low-salt' buffer [50 mM Tris-HCl, 1 mM NH_4Cl, 10 mM $MgCl_2$, 10 mM spermidine, 5% (w/v) poly(ethylene glycol) 8000, pH 7.2]. Archaeal RNase P reactions were performed at 55°C in 10 mM HEPES, 10 mM $Mg(CH_3CO_2)_2$, 800 mM $NH_4CH_3CO_2$, pH 7.2.

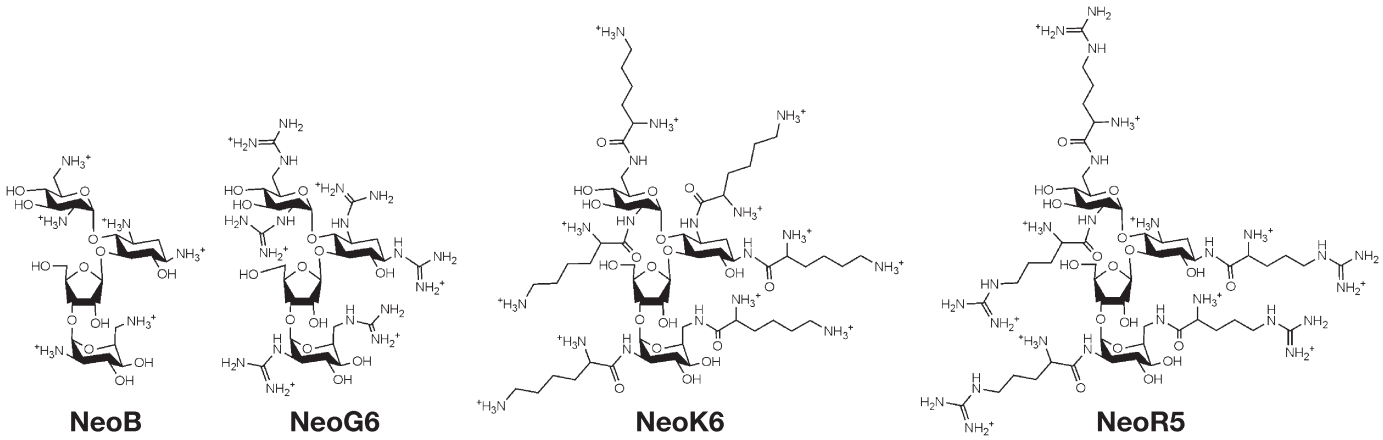

Figure 2. Structures of neomycin B (NeoB) and its guanidinium (NeoG6), lysyl (NeoK6) and argininyl (NeoR5) conjugates.

The reaction contents were separated on an 8% (w/v) polyacrylamide gel containing 7 M urea. The extent of substrate cleaved was visualized using a phosphorimager and quantitated with ImageQuant software (Molecular Dynamics).

The data in Figures 3B, 4B and 5D represent mean and standard deviation values calculated from at least three independent measurements of initial velocities for a given condition. Although the IC_{50} values, estimated from a plot of initial velocities versus inhibitor concentration, were reproducible, different batches of stock solutions did occasionally result in variations of up to 2-fold. Despite these differences, the inhibition curves unequivocally demonstrate the inhibitory trends with the various neomycin derivatives.

RESULTS

Rationale

Our first objective was to determine the structural aspects of NeoR6 that contributed to its nearly 500-fold increased potency compared to NeoB in inhibiting bacterial RNase P assayed in a 'low-salt' buffer (IC_{50} of 60 and 0.125 μM for NeoB and NeoR6, respectively; 17,26). To examine the effects of side-chain length, flexibility and composition, we replaced the Arg side chains with either guanidinium or lysyl moieties to yield NeoG6 or NeoK6, respectively (Figure 2). Our second objective was to inquire if these AG derivatives were either acting as peptidomimetics that affected bacterial RNase P holoenzyme assembly or disrupting catalytically essential divalent metal ions (Figure 1). The results of these studies are described below.

Synthesis of AG derivatives

Initially, we attempted to synthesize NeoR6 using published protocols (25) but were unsuccessful. Hence, we devised a different synthetic route that yielded not NeoR6 but a neomycin-penta-arginine conjugate (NeoR5; see 'Supplementary Data'). NeoR5 was used as the reference in our comparative studies with NeoK6 and NeoG6. While NeoK6 was synthesized using a new procedure (see 'Supplementary Data'), the synthesis of NeoG6 was based on methods already described (33–35). Elemental composition, NMR and mass spectrometric analyses unambiguously confirmed the identity of the end products.

Structure-activity relationships in AG-based inhibitors

We first define the expectations from a comparison of NeoR5 versus either NeoG6 or NeoK6. In NeoG6, the terminal guanidinuim groups in Arg are present albeit without the advantages of the length and flexibility afforded by the Arg side-chain and was therefore predicted to be a poorer inhibitor than NeoR5. Similarly, if the guanidinium functional groups in NeoR5 were involved in hydrogen bonding (in addition to ionic or π–π) interactions with RNase P, we postulated that replacing the planar guanidinium moieties in NeoR5 with protonated amines (as in NeoK6) should result in a decreased inhibitory potential despite NeoK6 fulfilling length and flexibility criteria.

When we assayed the *E. coli* RNase P holoenzyme in a 'high-salt buffer' in the absence and presence of 2.5 μM of the various neomycin derivatives, NeoR5 was clearly a more potent inhibitor than NeoG6 or NeoK6 (Figure 3A, lanes 2–5). The importance of the AG backbone was also borne out by the finding that addition of 1 mM arginine, lysine or guanidine to the assay had no effect on the *E. coli* RNase P holoenzyme activity (Figure 3A, lanes 6–8). To calculate the IC_{50} values, we determined the initial velocities in the absence and presence of various concentrations of NeoB (the parental AG), NeoG6, NeoK6 and NeoR5. The IC_{50} values are ~400, 6, 3 and 0.5 μM for NeoB, NeoG6, NeoK6 and NeoR5, respectively (Figure 3B). The trends observed are discussed in detail later.

Mechanism of action of AG derivatives

There are at least two major strategies for inhibiting bacterial RNase P (Figure 1; 9). The first approach is to disrupt formation of the holoenzyme (i.e. RNP complex) by displacing or preventing the binding of the protein cofactor to the catalytic RNA moiety. Such compounds

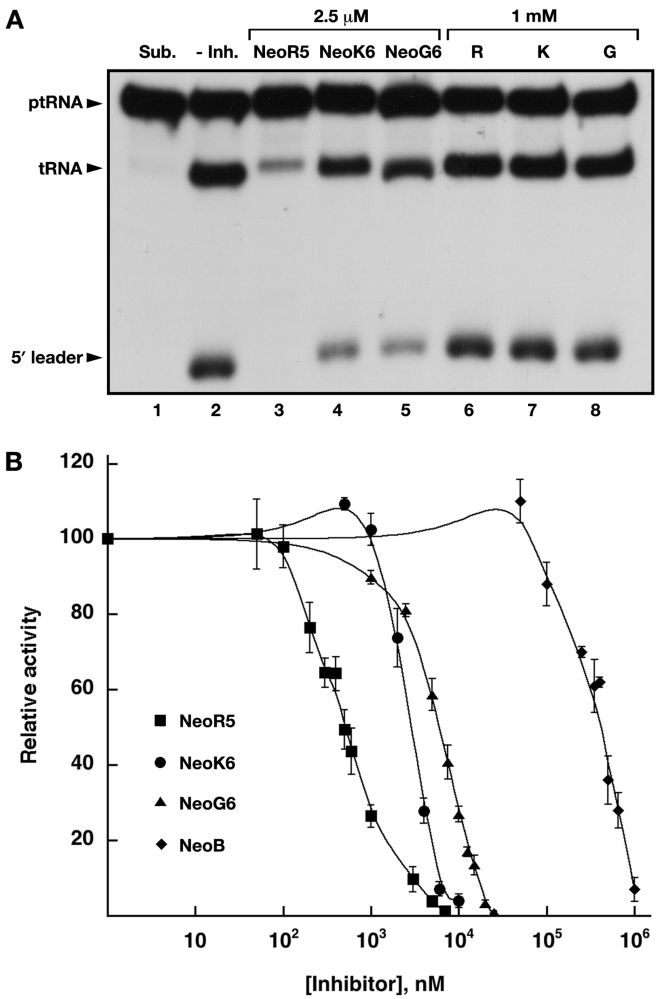

Figure 3. Inhibition of bacterial RNase P by different neomycin B derivatives. (**A**) Inhibition of *in vitro* reconstituted *E. coli* RNase P by NeoR5, NeoK6 or NeoG6. As controls, free arginine (R), lysine (K) and guanidine (G) were also tested. The lanes labeled 'Sub.' and '-Inh.' indicate $ptRNA^{Tyr}$ substrate that was incubated without any inhibitor in the absence and presence of *E. coli* RNase P, respectively. (**B**) Estimation of IC_{50} values for inhibition of *E. coli* RNase P by NeoR5, NeoK6, NeoG6 and NeoB. The ptRNA processing activity observed with a given concentration of the inhibitor is presented as relative activity by using the activity observed without the inhibitor as reference.

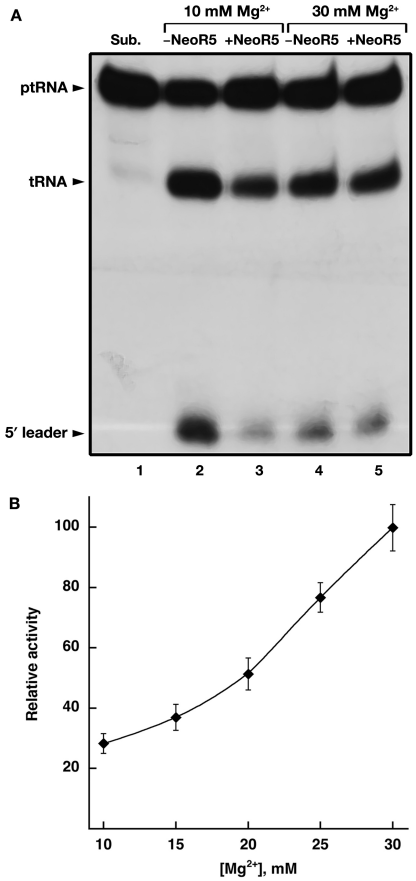

Figure 4. Mg^{2+}-mediated rescue of NeoR5 inhibition of bacterial RNase P. (**A**) Lack of inhibition of *E. coli* RNase P by 1 μM NeoR5 in the presence of 30 mM Mg^{2+} (as compared to 10 mM Mg^{2+}). The lane labeled 'Sub.' indicates $ptRNA^{Tyr}$ substrate that was incubated in the absence of any enzyme or inhibitor. (**B**) Gradual rescue of NeoR5 inhibition by increasing the concentration of Mg^{2+} in the assay. Since bacterial RNase P holoenzyme activity decreases with increasing Mg^{2+}, the relative activity presented refers to the ptRNA processing activity observed in the presence of NeoR5 compared to that in its absence at the specified Mg^{2+} concentration.

(class I inhibitors) would include peptidomimetics that might compete with the protein cofactor for binding the RNA subunit. A compound that binds the RNA subunit allosterically and changes its conformation, thereby rendering it inaccessible for binding by the protein cofactor, would also merit inclusion in this category. The second approach involves using class II inhibitors to interfere with RNase P catalysis, either by displacing Mg^{2+} ions required for catalysis or by preventing ptRNA substrate binding. At the conclusion of our previous study (26), we were unsure which of the above-mentioned routes were employed by AACs in inhibiting *E. coli* RNase P.

It is important to note that we did eliminate the possibility that non-specific interactions of AACs with the ptRNA substrate affect its processing by RNase P. When we either included competitor RNAs (e.g. polyA) or increased the concentration of the ptRNA substrate in the assay, we found that these changes did not affect the inhibitory potential of AACs (26).

Since Litovchick *et al.* (24) reported that AACs inhibit the binding of Tat protein to various targets, including TAR RNA, probably by mimicking the conserved binding motif ($R_{49}KKRRQRRR_{57}$) of the Tat protein, it seemed possible that AACs, with their multiple Arg side chains, could also mimic the conserved Arg residues in the α2-helix of the bacterial RPP (36) and disrupt bacterial RNase P holoenzyme assembly (9). We sought to test this idea using stocks of AACs generously provided by Prof. Aviva Lapidot, Weizmann Institute of Science. However, protein rescue and RNase T1/V1 protection experiments did not support this hypothesis (data not shown; 37). Increasing the concentration of *E. coli* RPP did not rescue *E. coli* RNase P activity from inhibition by AACs. Also, the *E. coli* RPP's footprint on its cognate RPR, as assessed from protection of the RPR from cleavage by RNase T1/V1, remained unchanged upon addition of AACs (data not shown; 37). Taken together, we conclude that AACs

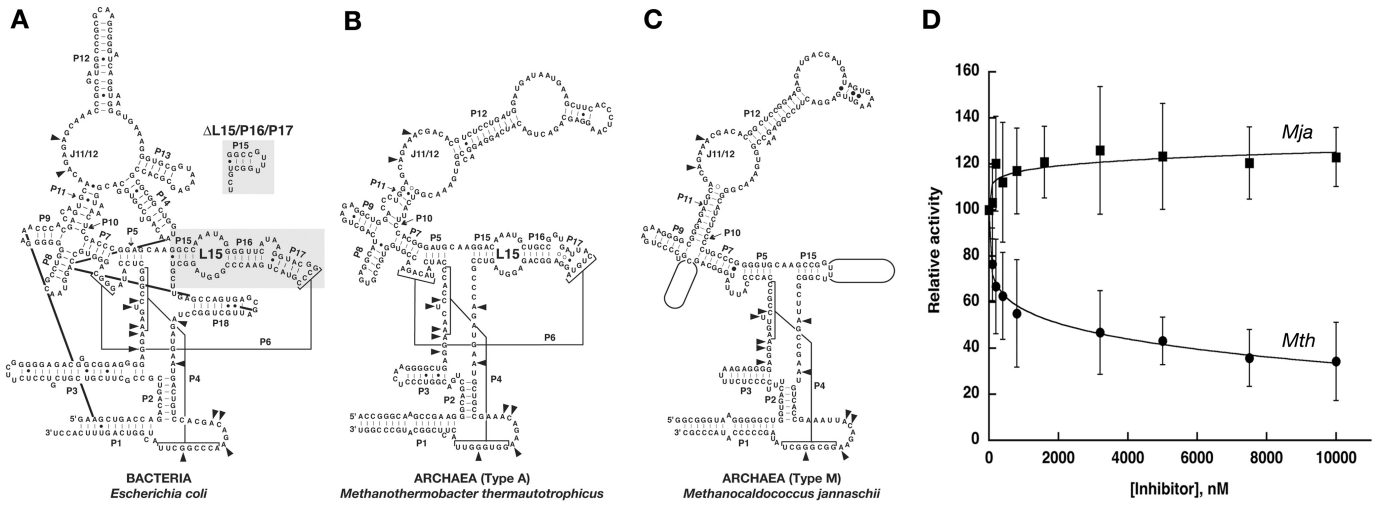

Figure 5. Differential inhibition of archaeal RNase P by NeoR5. (**A**, **B**, and **C**) Secondary structure depictions of representative bacterial and archaeal RPRs; arrowheads indicate universally conserved nucleotides (50). Helices (or paired regions) are labeled as P1, P2, etc., consecutively from 5′ to 3′; linkers are denoted as joining regions (e.g. J11/12 as the connector between P11 and P12); the L15 loop is specifically indicated. In panel C, the empty boxes represent the structural elements that are absent in the type M archaeal RPR. (**D**) Inhibition of type A (*Mth*) and M (*Mja*) archaeal RNase P by NeoR5. The ptRNA processing activity observed with a given concentration of the inhibitor is presented as relative activity by using the activity observed without the inhibitor as reference.

do not compete with the protein cofactor for binding to the RNA subunit.

RNase P-mediated cleavage is believed to occur via an S_N2 reaction in which a metal-hydroxide nucleophile attacks the scissile phosphodiester linkage (5). Since AACs do not disrupt bacterial RNase P holoenzyme formation, we investigated whether AACs interfere with binding of Mg^{2+} ions critical for catalysis. It has been noted that NeoB interferes with the binding of Mg^{2+} ions to *E. coli* RPR, the catalytic RNA moiety of *E. coli* RNase P (17,38); this strategy also applies to inhibition of the group I intron by NeoB (39). Our results demonstrate that raising the concentration of Mg^{2+} in the assay does rescue *E. coli* RNase P from inhibition by NeoR5 (Figure 4A). In the presence of 1 μM NeoR5 and 10 mM Mg^{2+}, there is marked inhibition of *E. coli* RNase P activity; in contrast, 1 μM NeoR5 has almost no effect at 30 mM Mg^{2+}. Note that activity of *E. coli* RNase P is lower at 30 mM compared to 10 mM Mg^{2+}, reflecting the decrease in bacterial RNase P holoenyzme activity with increasing Mg^{2+} (37).

By calculating the initial velocities of *E. coli* RNase P at increasing Mg^{2+} concentrations (from 10 to 30 mM) in the absence and presence of 0.5 μM NeoR5, we were able to demonstrate that progressively increasing the concentration of Mg^{2+} in the assay completely eliminates inhibition of *E. coli* RNase P by NeoR5 (Figure 4B). Similar rescue trends were observed when NeoG6 and NeoK6 were used as inhibitors of *E. coli* RNase P and the concentration of Mg^{2+} in the assay gradually increased (data not shown; 37).

Specificity of targeting

Displacement of Mg^{2+} in the *E. coli* RNase P holoenzyme (136 kDa) by NeoR5 (1.4 kDa) is pivotal to the latter's ability to be a potent inhibitor. It is possible that these critical metal ions are positioned at specific locations in the RPR's tertiary structure and that the potency of a given inhibitor is related to its shape/charge complementarity with the Mg^{2+}-binding site(s) in the RPR. A corollary would be that RNase P in the three domains of life, with its varying RNP composition and structures, might display differential susceptibility to NeoR5. Indeed, this is the case.

Archaeal RNase P holoenzymes are made up of an essential RPR and at least four RPPs, the latter initially identified by mining databases of archaeal genome sequences with eukaryal RPPs serving as queries (5–8). Euryarchaeal RPRs have been classified into types A and M based on secondary structure variations such as the absence of a paired region P8 or a large L15 loop (Figure 5B versus 5C; 40). We have recently succeeded in reconstituting both type A and M archaeal RNase P holoenzymes *in vitro* using recombinant subunits (29–31; Pulukkunat *et al.*, in preparation) and have demonstrated robust ptRNA-processing activities. Since the archaeal RNase P holoenzymes are typically assayed at 55°C in contrast to the assay temperature of 37°C used for *E. coli* RNase P, we first tested the ability of NeoR5 to inhibit *E. coli* RNase P at 55°C and found that the IC_{50} value was unchanged from that calculated at 37°C (data not shown). We then used *in vitro* reconstituted *Mth* and *Mja* RNase P holoenzymes, as representatives of type A and M archaeal RNase P, respectively, and examined their susceptibility to inhibition by NeoR5. When we measured the initial velocities of *Mth* and *Mja* RNase P in the absence and presence of increasing concentrations of NeoR5, marked differences became evident (Figure 5D). *Mth* RNase P was inhibited quite significantly and progressively up to 10 μM NeoR5 (similar inhibition by NeoR5 was found with another type A RNase P from *Pyrococcus furiosus*; data not shown). In stark contrast, *Mja* (type M) RNase P was activated modestly (Figure 5D). This activation could be due to stabilization of RNA structure for which there

is precedent (41); in the absence of metal ions, both polyamines and NeoB are known to promote hairpin ribozyme cleavage perhaps by acting as surrogates for metal ions (42).

The above results with type A and M archaeal RNase P were somewhat expected since the L15 loop of *E. coli* RNase P (Figure 5A), which is significantly diminished in type M (*Mja*) RNase P (Figure 5C), has been shown to be important for inhibition by NeoB (17). Mutations in the *E. coli* RPR's L15 loop, that weaken Mg^{2+} binding to L15, resulted in a 3-fold increase in the IC_{50} for NeoB (17). We therefore inquired if deleting L15 (and the P16/P17 stems) would result in an *E. coli* RPR that would be less susceptible to inhibition by NeoR5. Intriguingly, such an *E. coli* RPR mutant (ΔL15/P16/P17; Figure 5A), when reconstituted with the *E. coli* Rpp to generate a holoenzyme, was indistinguishable from its wild-type counterpart in terms of turnover number and inhibition by NeoR5 (IC_{50}~0.5 μM; data not shown). This result indicates that the mutant RPR must somehow offer an alternative binding site(s) for NeoR5 that still permits its interference with RNase P function. This also illustrates the caveat of using deletion-based approaches to map binding sites in RNAs for AGs and AACs, opportunistic ligands that are adept at finding new binding pockets in target RNAs (13).

DISCUSSION

Structure–activity relationships in AG derivatives that inhibit bacterial RNase P

To rationalize the enhanced potency of NeoR5 compared to NeoB in inhibiting bacterial RNase P activity (26), we synthesized penta-argininyl (NeoR5), hexa-lysyl (NeoK6) and hexa-guanidinium (NeoG6) conjugates of NeoB and then determined how their ability to inhibit *E. coli* RNase P is influenced by the characteristics of the side chains attached to the neomycin backbone. Our studies revealed that NeoR5 was the most potent inhibitor having an IC_{50} ~ 0.5 μM. Under identical assay conditions, both NeoK6 and NeoG6 were ~10-fold weaker while NeoB was ~800-fold weaker than NeoR5 (Figure 3B).

We infer that the potency of NeoR5 does not stem from a single structural characteristic but instead is due to a combination of side-chain length, flexibility and composition. The importance of side-chain length and flexibility is demonstrated by comparing NeoR5 with NeoG6, in which the side chains are shortened to only the guanidinium functional groups present in the Arg termini of NeoR5 (Figure 2). Likewise, NeoK6 demonstrates the importance of side-chain composition; its Lys residues, with roughly the same side-chain length as Arg, have terminal protonated amines but lack the guanidinium moieties (Figure 2). NeoG6 and NeoK6 are both 10-fold weaker than NeoR5 indicating that the Arg side chains in NeoR5 are possibly involved in hydrogen bonding (and possibly π–π interactions) in addition to electrostatic interactions. Such a premise is consistent with the finding that inhibition by Arg conjugates of neomycin exhibit very weak salt dependence compared to NeoB; for instance, the IC_{50} for inhibition of *E. coli* RNase P by NeoB increases 7-fold when the assay is performed in a 'high-salt' instead of a 'low-salt' buffer (37).

While the nature of the moieties attached to AGs clearly contributes to fine tuning the inhibitory potency, the parental backbone also plays a crucial role. AGs bind RNAs by virtue of electrostatic and hydrogen bonding interactions, and therefore some target specificity could be expected when AGs with different backbone structures and geometries are compared. This notion has indeed been borne out in studies with RNase P. For instance, NeoB and paromomycin (Par) differ only by a single substitution of a hydroxyl group in NeoB for an amino group in Par, yet this subtle difference results in Par being 6-fold weaker than NeoB in inhibiting bacterial RPR (17). Thus, while designing new AG conjugates, backbone variations must also be considered.

Mechanism of inhibition of bacterial RNase P by AG conjugates

AGs successfully interfere with the function of a target RNA by either displacing metal ions or altering structure. The inhibition of *E. coli* RPR activity by NeoB is suppressed at high concentration of Mg^{2+} and at high pH where the amino groups in the AGs are not protonated (17,37). Hence, the inhibitory potential of AGs has been attributed to their ability to displace Mg^{2+} ions, essential for RNase P catalysis, from high affinity binding sites in the RPR; parallels have been proposed to account for the ability of AGs to inhibit other ribozymes and even nucleic acid-metabolizing protein enzymes that possess negatively charged pockets (39,43).

While such a mechanism of action seems likely for NeoR5, we also entertained the idea that the Arg side-chains splayed out from the neomycin backbone might render NeoR5 a potent peptidomimic that could compete with the bacterial RPP for binding to its cognate RPR and thereby disrupt assembly of the bacterial RNase P holoenzyme (i.e. a class I inhibitor in the scheme depicted in Figure 1). Such a possibility seemed reasonable in light of the clustering of conserved and functionally important Arg residues in a single α-helix of bacterial RPP (36). However, increasing the concentration of bacterial RPP did not abolish inhibition of bacterial RNase P by AACs. Also, footprinting studies probing RNP interactions in the bacterial RNase P holoenzyme, in the absence and presence of AACs, revealed that AACs do not dislodge the RPP from the holoenzyme. These findings then left us with the recurring mechanistic theme that AACs, like AGs, might function by displacing metal ions from RNase P. Indeed, Mg^{2+} rescue experiments demonstrated that the inhibition of *E. coli* RNase P by NeoR5 was completely reversed by increasing Mg^{2+} from 10 to 30 mM in the assay (Figure 4).

Displacement of Mg^{2+} by NeoR5 could inhibit RNase P by affecting RPR folding, ptRNA binding, or the hydrolytic cleavage step. This mechanistic basis remains to

be delineated. A photochemical crosslinking or footprinting strategy using a derivatized NeoR5 would help map its binding site(s) on bacterial and archaeal RPRs and thereby shed light on its mechanism of inhibition of *E. coli* RNase P. In the absence of such information, we can only speculate on its binding site(s).

Site-specific cleavages in the *E. coli* RPR mediated by metal ions have been used to deduce the possible location of metal ion-binding sites such as the L15 loop (44). Interestingly, the inhibition of *E. coli* RPR by NeoB was ascribed (at least in part) to its ability to displace Mg^{2+} ions from L15; this inference was based on the modestly decreased susceptibility of L15 mutants to inhibition by NeoB and to lead-induced cleavage (17). L15 in the bacterial RPR plays a role in substrate recognition, cleavage site selection and metal ion binding (45); however, we do not know if Mg^{2+} ions bound to L15 are directly involved in cleavage of the scissile phosphodiester linkage in the ptRNA substrate. The tertiary structures of bacterial RPRs (46,47) illustrate the exquisite tertiary interactions and overall folds but, in the absence of a substrate, they did not reveal (as expected) the locations of the metal ions essential for catalysis. Nevertheless, there is growing biochemical evidence that Mg^{2+} ions bound to L15 are part of a metal ion cluster that dictates the positioning of the catalytic metal ions (45). Although we do not have direct evidence to suggest that NeoR5 inhibits *E. coli* RNase P by binding to L15, some support for this notion stems from the failure of NeoR5 to inhibit an archaeal RNase P lacking the typical L15 and the attached stems (Figure 5C). However, this idea needs to be tempered by our finding that NeoR5 inhibits *E. coli* RNase P ΔL15/P16/P17 mutant as effectively as it inhibits the wild type. Given the opportunistic behavior of AGs (and possibly AACs), this result does not conclusively eliminate the possibility of NeoR5 binding to L15 in the wild-type *E. coli* RNase P (see below).

Selectivity

Moderate/high affinity and high selectivity for the target RNA are essential attributes that are expected of small molecules designed to interfere with RNA function (1–4,13). AGs do not fulfill these criteria as borne out by various studies. First, the availability of multiple binding sites in a target RNA, or the presence of a fortuitous site in an unintended RNA that might offer nearly ideal electrostatic complementarity to accommodate the AG ligands, makes it difficult to ensure high specificity. In fact, this type of binding flexibility in the *E. coli* RPR might underlie the ability of NeoR5 to inhibit the *E. coli* RNase P holoenzyme reconstituted with either the wild-type RPR or the ΔL15/P16/P17 RPR, in which the putative primary binding site for AGs is missing. Second, high-resolution structural studies illustrate the plasticity of AGs in adopting two different conformations while binding two distinct RNA targets (13).

Although the striking adaptability of AGs as RNA ligands undermines their usage with high selectivity, modifications to AGs have improved both affinity and specificity (13,21). In this study, we observed that NeoR5 can distinguish between type A and M archaeal RNase P (Figure 5), a somewhat unexpected result since both holoenzymes were reconstituted with an RPR and four RPPs, which share sequence and structure homology. While the type M RPRs are smaller by ~10% relative to the type A counterparts, the reconstituted holoenzymes are roughly the same size. Furthermore, the presence of 12 or so universally conserved nucleotides at nearly identical locations in the RPRs from all three domains of life suggests a common RNA-mediated catalytic reaction in all RNase P holoenzymes and implies that the ability of NeoR5 to discriminate among them stems from structural considerations rather than differences in catalytic mechanisms. Even subtle variations in the RPR structure, especially in the context of a different suite of RPR–RPP interactions in the respective RNase P holoenzyme, would influence the number, location and affinity of metal-ion binding sites which in turn would affect the susceptibility to NeoR5. Another observation highlighting the selectivity of AACs is the ability of NeoR6 to discriminate between the eukaryal and the bacterial translational machinery (48). Taken together, we expect that the availability of the tertiary structures of RNase P from the three domains of life might yet allow design of AG conjugates that are highly selective for bacterial RNase P.

SUPPLEMENTARY DATA

Supplementary Data are available at NAR Online.

ACKNOWLEDGEMENTS

This work was supported by grants from the National Science Foundation to V.G. (MCB 0091081), National Institutes of Health to Mark P. Foster and V.G. (R01 GM067807) and by an NSF REU Award to support S.A.K. (REU supplement to MCB 0091081). We are indebted to Prof. Yitzhak Tor, University of California, San Diego, for providing advice on the preparation of reagents and for discussions, and to Prof. Aviva Lapidot, Weizmann Institute of Science, Israel, for generously providing AACs that were used in some of our earlier studies. We are grateful to members of the Gopalan laboratory for providing helpful suggestions and valuable reagents for this study. We thank Lien Lai for her critical comments on the manuscript. Funding to pay the Open Access publication charges for this article was provided by an anonymous private donor.

Conflict of interest statement. None declared.

REFERENCES

1. Gallego,J. and Varani,G. (2001) Targeting RNA with small-molecule drugs: Therapeutic promise and chemical challenges. *Acc. Chem. Res.*, **34**, 836–843.
2. Hermann,T. (2003) Chemical and functional diversity of small molecule ligands for RNA. *Biopolymers*, **70**, 4–18.
3. Hermann,T. and Tor,Y. (2005) RNA as target for small molecule therapeutics. *Expert Opin. Ther. Patents*, **15**, 49–62.

4. Silva,J.G. and Carvalho,I. (2007) New insights into aminoglycoside antibiotics and derivatives. *Curr. Med. Chem.*, **14**, 1101–1119.
5. Hall,T.A. and Brown,J.W. (2001) The ribonuclease P family. *Meth. Enzymol.*, **341**, 56–77.
6. Evans,D., Marquez,S.M. and Pace,N.R. (2006) RNase P: interface of the RNA and protein worlds. *Trends Biochem. Sci.*, **31**, 333–341.
7. Gopalan,V. and Altman,S. (2006) Ribonuclease P: structure and catalysis. In Gesteland,R.F., Cech,T. and Atkins,J.F. (eds), *The RNA World*. Cold Spring Harbor Laboratory Press, Cold Spring Harbor, NYChapter 6.1 (online only at http://rna.cshl.edu).
8. Walker,S.C. and Engelke,D.R. (2006) Ribonuclease P: the evolution of an ancient RNA enzyme. *Crit. Rev. Biochem. Mol. Biol.*, **41**, 77–102.
9. Eder,P.S., Hatfield,C., Vioque,A. and Gopalan,V. (2003) Bacterial RNase P as a potential target for novel anti-infectives. *Curr. Opin. Invest. Drugs.*, **4**, 937–943.
10. Willkomm,D.K., Gruegelsiepe,H., Goudinakis,O., Kretschmer-Kazemi Far,R., Bald,R., Erdmann,V.A. and Hartmann,R.K. (2003) Evaluation of bacterial RNase P as a drug target. *ChemBioChem.*, **4**, 1041–1048.
11. Dahlberg,A.E., Horodyski,F. and Keller,P. (1978) Interaction of neomycin with ribosomes and ribosomal ribonucleic acid. *Antimicrob. Agents Chemother.*, **13**, 331–339.
12. Moazed,D. and Noller,H.F. (1987) Interactions of antibiotics with functional sites in 16S ribosomal RNA. *Nature*, **327**, 389–394.
13. Tor,Y. (2006) The ribosomal A-site as an inspiration for the design of RNA binders. *Biochimie*, **88**, 1045–1051.
14. Zapp,M.L., Stern,S. and Green,M.R. (1993) Small molecules that selectively block RNA binding of HIV-1 Rev protein inhibit Rev function and viral production. *Cell*, **74**, 969–978.
15. von Ahsen,U., Davies,J. and Schroeder,R. (1991) Antibiotic inhibition of group I ribozyme function. *Nature*, **353**, 368–370.
16. Rogers,J., Chang,A.H., von Ahsen,U., Schroeder,R. and Davies,J. (1996) Inhibition of the self-cleaving reaction of the human Hepatitis delta virus ribozyme by antibiotics. *J. Mol. Biol.*, **259**, 916–925.
17. Mikkelsen,N.E., Brännvall,M., Virtanen,A. and Kirsebom,L. (1999) Inhibition of RNase P RNA cleavage by AGs. *Proc. Natl Acad. Sci. USA*, **96**, 6155–6160.
18. Hermann,T. and Westhof,E. (1998) Aminoglycoside binding to the hammerhead ribozyme: a general model for the interaction of cationic antibiotics with RNA. *J. Mol. Biol.*, **276**, 903–912.
19. Tor,Y., Hermann,T. and Westhof,E. (1998) Deciphering RNA recognition: aminoglycoside binding to the hammerhead ribozyme. *Chem. Biol.*, **5**, R277–283.
20. Vicens,Q. and Westhof,E. (2003) Molecular recognition of aminoglycoside antibiotics by ribosomal RNA and resistance enzymes: an analysis of X-ray crystal structures. *Biopolymers*, **70**, 42–57.
21. Leudtke,N.W., Baker,T.J., Goodman,M. and Tor,Y. (2000) Guanidinoglycosides: a novel family of RNA ligands. *J. Am. Chem. Soc.*, **122**, 12035–12036.
22. Tan,R. and Frankel,A.D. (1995) Structural variety of arginine-rich RNA binding peptides. *Proc. Natl Acad. Sci. USA*, **92**, 5282–5286.
23. Puglisi,J.D., Chen,L., Blanchard,S. and Frankel,A.D. (1995) Solution structure of a bovine immunodeficiency virus Tat-TAR peptide-RNA complex. *Science*, **270**, 1200–1203.
24. Litovchick,A., Evdokimov,A.G. and Lapidot,A. (2000) Arginine-aminoglycoside conjugates that bind to HIV transactivation responsive element RNA *in vitro*. *Biochemistry*, **39**, 2838–2852.
25. Litovchick,A., Lapidot,A., Eisenstein,M., Kalinkovich,A. and Borkow,G. (2001) Neomycin B-arginine conjugate, a novel HIV-1 Tat antagonist: synthesis and anti-HIV activities. *Biochemistry*, **40**, 15612–15623.
26. Eubank,T.D., Biswas,R., Jovanovic,M., Litovchick,A., Lapidot,A. and Gopalan,V. (2002) Inhibition of bacterial RNase P by aminoglycoside-arginine conjugates. *FEBS Lett.*, **511**, 107–112.
27. Kawamato,S.A. (2004) Elucidating structure-activity relationships and the mechanism of inhibition of bacterial RNase P by aminoglycoside derivatives. B.S. (Honors) Thesis, The Ohio State University, Columbus, OH, USA.
28. Vioque,A., Arnez,J. and Altman,S. (1988) Protein-RNA interactions in the RNase P holoenzyme from *Escherichia coli*. *J. Mol. Biol.*, **202**, 835–848.
29. Boomershine,W.P., McElroy,C.A., Tsai,H.Y., Wilson,R.C., Gopalan,V. and Foster,M.P. (2003) Structure of Mth11/Mth Rpp29, an essential protein subunit of archaeal and eukaryotic RNase P. *Proc. Natl Acad. Sci. USA*, **100**, 15398–15403.
30. Tsai,H.Y., Pulukkunat,D.K., Woznick,W. and Gopalan,V. (2006) Functional reconstitution and characterization of *Pyrococcus furiosus* RNase P. *Proc. Natl Acad. Sci. USA*, **103**, 16147–16152.
31. Zhu,Y., Pulukkunat,D.K. and Li,Y. (2007) Deciphering RNA structural diversity and systematic phylogeny from microbial metagenomes. *Nucleic Acids Res.*, **35**, 2283–2294.
32. Zahler,N.H., Christian,E.L. and Harris,M.E. (2003) Recognition of the 5′ leader of pre-tRNA substrates by the active site of ribonuclease P. *RNA*, **9**, 734–745.
33. Baker,T.J., Tomioka,M. and Goodman,M. (2000) Preparation and use of N,N′-di-Boc-N″-triflylguanidine. *Org. Syn.*, **78**, 91–98.
34. Baker,T.J., Luedtke,N.W., Tor,Y. and Goodman,M. (2000) Synthesis and anti-HIV activity of guanidinoglycosides. *J. Org. Chem.*, **65**, 9054–9058.
35. Hui,Y., Ptak,R., Paulman,R., Pallansch,M. and Chang,C.W.T. (2002) Syntheis of novel guanidine incorporated AGs, guanidino-pyranamycins. *Tetrahedron Lett.*, **43**, 9255–9257.
36. Jovanovic,M., Sanchez,R., Altman,S. and Gopalan,V. (2002) Elucidation of structure-function relationships in the protein subunit of bacterial RNase P using a genetic complementation approach. *Nucleic Acids Res.*, **22**, 4087–4094.
37. Hatfield,C.L. (2004) Elucidating the mechanism of inhibition of bacterial RNase P by aminoglycoside derivatives. M.S. Thesis, Department of Biochemistry, The Ohio State University, Columbus, OH, USA.
38. Mikkelsen,N.E., Johansson,K., Virtanen,A. and Kirsebom,L.A. (2001) Aminoglycoside binding displaces a divalent metal ion in a tRNA-neomycin B complex. *Nature Struct. Biol.*, **8**, 510–514.
39. Hoch,I., Berens,C., Westhof,E. and Schroeder,R. (1998) Antibiotic inhibition of RNA catalysis: neomycin B binds to the catalytic core of the *td* group I intron displacing essential metal ions. *J. Mol. Biol.*, **282**, 557–569.
40. Harris,J.K., Haas,E.S., Williams,D.A. and Brown,J.W. (2001) New insights into RNase P RNA structure from comparative analysis of the archaeal RNA. *RNA*, **7**, 220–232.
41. Arya,D., Xue,L. and Willis,B. (2003) Aminoglycoside (neomycin) preference is for A-form nucleic acids, not just RNA: results from a competition dialysis study. *J. Am. Chem. Soc.*, **125**, 10148–10149.
42. Earnshaw,D.J. and Gait,M.J. (1998) Hairpin ribozyme cleavage catalyzed by aminoglycoside antibiotics and the polyamine spermine in the absence of metal ions. *Nucleic Acids Res.*, **26**, 5561–5571.
43. Thuresson,A.-C., Kirsebom,L.A. and Virtanen,A. (2007) Inhibition of polyA polymerase by AGs. *Biochimie*, **89**, 1221–1227.
44. Kazakov,S. and Altman,S. (1991) Site-specific cleavage by metal ion cofactors and inhibitors of M1 RNA, the catalytic subunit of RNase P from *Escherichia coli*. *Proc. Natl Acad. Sci. USA*, **88**, 9193–9197.
45. Kirsebom,L.A. (2007) RNase P RNA mediated cleavage: substrate recognition and catalysis. *Biochimie*, **89**, 1183–1194.
46. Torres-Larios,A., Swinger,K.K., Krasilnikov,A.S., Pan,T. and Mondragon,A. (2005) Crystal structure of the RNA component of bacterial ribonuclease P. *Nature*, **437**, 584–587.
47. Kazantsev,A.V., Krivenko,A.A., Harrington,D.J., Holbrook,S.R., Adams,P.D. and Pace,N.R. (2005) Crystal structure of a bacterial ribonuclease P RNA. *Proc. Natl Acad. Sci. USA*, **102**, 13392–13397.
48. Carriere,M., Vijayabaskar,V., Applefield,D., Harvey,I., Garneau,P., Lorsch,J., Lapidot,A. and Pelletier,J. (2002) Inhibition of protein synthesis by aminoglycoside-arginine conjugates. *RNA*, **8**, 1267–1279.
49. Christian,E.L., Zahler,N.H., Kaye,N.M. and Harris,M.E. (2002) Analysis of substrate recognition by the ribonucleoprotein endonuclease RNase P. *Methods*, **28**, 307–322.
50. Brown,J.W. (1999) The ribonuclease P database. *Nucleic Acids Res.*, **27**, 314.